

## Motorcycle simulator subjective and objective validation for low speed maneuvering

Grottoli, Marco; Mulder, Max; Happee, Riender

**DOI**

[10.1177/09544070221110930](https://doi.org/10.1177/09544070221110930)

**Publication date**

2022

**Document Version**

Final published version

**Published in**

Proceedings of the Institution of Mechanical Engineers, Part D: Journal of Automobile Engineering

**Citation (APA)**

Grottoli, M., Mulder, M., & Happee, R. (2022). Motorcycle simulator subjective and objective validation for low speed maneuvering. *Proceedings of the Institution of Mechanical Engineers, Part D: Journal of Automobile Engineering*, 237 (2023)(9), 2175-2189. <https://doi.org/10.1177/09544070221110930>

**Important note**

To cite this publication, please use the final published version (if applicable).  
Please check the document version above.

**Copyright**

Other than for strictly personal use, it is not permitted to download, forward or distribute the text or part of it, without the consent of the author(s) and/or copyright holder(s), unless the work is under an open content license such as Creative Commons.

**Takedown policy**

Please contact us and provide details if you believe this document breaches copyrights.  
We will remove access to the work immediately and investigate your claim.

# Motorcycle simulator subjective and objective validation for low speed maneuvering

Marco Grottoli<sup>1,2</sup> , Max Mulder<sup>1</sup> and Riender Happee<sup>1</sup>

Proc IMechE Part D:  
J Automobile Engineering  
2023, Vol. 237(9) 2175–2189  
© IMechE 2022



Article reuse guidelines:

sagepub.com/journals-permissions  
DOI: 10.1177/09544070221110930  
journals.sagepub.com/home/pid



## Abstract

The use of driving simulators for training and for development of new vehicles is widely spread in the automotive industry. In the last decade, a few motorcycle riding simulators have been developed for similar purposes, with focus on maneuvering at high speed. This article presents the subjective and objective evaluation of a motorcycle riding simulator specifically for low speed longitudinal and lateral maneuvering, between 0 and 10 ms<sup>-1</sup>. An experiment was conducted with and without platform motion, focusing on three maneuvers: acceleration from standstill, braking to standstill and turning at constant speed. Participants briefly evaluated the fidelity of the simulator after each maneuver and more extensively after each motion condition. Behavioral fidelity was evaluated using experimental data measured on an instrumented motorcycle. Overall, the results show that the participants could reproduce the selected maneuvers without falling or losing balance, reporting a sufficient level of simulator realism. In terms of subjective fidelity, platform motion had a positive effect on simulator presence, significantly increasing the feeling of being involved in the virtual environment. In terms of behavioral fidelity, the comparison between the simulator and experimental results shows good agreement, with a limited positive influence of motion for the braking maneuver, which indicates that for this maneuver the use of motion is beneficial to reproduce the real-life experience and performance.

## Keywords

Motorcycle, simulator, validation

Date received: 4 October 2021; accepted: 18 May 2022

## Introduction

Diving simulators are widely used in the automotive industries, with applications ranging from driver training and testing of active safety systems, to the analysis of vehicle design modifications and subjective vehicle performance assessment. Simulators are also great tools to study the human vehicle interaction safely and repeatably. Applications are generally limited to cars, however, and the technology is rarely used for motorcycles. Due to the complex dynamics of two-wheeled vehicles, the use of a motorcycle riding simulator would be beneficial to train riders to cope with vehicle instabilities, and simulators could also be used to evaluate design changes and the impact of active safety systems. However, the complex dynamics of motorcycles also pose unique challenges for the design of realistic, high fidelity, simulators.

The fidelity of a simulator partly depends on the quality of the vehicle dynamics model, as this is the basis for rendering the visual stimuli as well as haptic

and motion cueing.<sup>1,2</sup> This topic was addressed in Grottoli et al.,<sup>3</sup> where a high fidelity model of a motorcycle was developed based on multibody dynamics theory. The dynamic model is used together with models of motorcycle sub-systems for engine, Continuously Variable Transmission (CVT), brakes, and tires. The presented model was validated for a selection of longitudinal and lateral dynamic maneuvers with experimental results in the speed range currently of interest, namely between 0 and 10 ms<sup>-1</sup>. Despite its complexity, the model can be simulated in real-time and in Kováčová et al.<sup>4</sup> it was integrated in a riding simulator for a study on braking at intersections. In that study,

<sup>1</sup>Delft University of Technology, Delft, The Netherlands

<sup>2</sup>Siemens Digital Industries Software, Leuven, Belgium

### Corresponding author:

Marco Grottoli, Faculty of 3mE (BMechE), Delft University of Technology, Mekelweg 2, Delft 2628 CD, The Netherlands.

Email: m.grottoli@tudelft.nl

the motorcycle model was simplified for the use in longitudinal direction only, introducing dynamic constraints that allowed the dynamic model to move only in fore-aft, vertical and pitch direction. Positive effects were found for usability and perceived realism with limited beneficial effects of platform motion. As a next step, the current study aims to validate the use of the motorcycle model for combined longitudinal and lateral dynamics.

The output of the motorcycle model simulation provides the reference motion that needs to be presented to the simulator rider as realistically as possible. This introduces challenges for the reproduction of motion, visual, and haptic cues. A particular challenge in simulators of two-wheeled vehicles is the rendering of roll motion in response to steering. In previous studies, different methods have been adopted to render roll motion. In all these studies, a combination of physical and visual stimuli is used to create perception of roll motion. In Kageyama,<sup>5</sup> a gain was tuned on both physical motion and visual roll, to find the optimal subjective compromise during an experiment with four participants. Results showed that participants preferred a larger physical roll (250% of the vehicle roll) rather than visual roll (119% of the vehicle roll). In another motorcycle simulator study,<sup>6</sup> the opposite approach was used, where a larger visual roll was presented to the simulator riders and only a small part of the vehicle roll was rendered using the physical tilting of the mock-up. In Guth et al.,<sup>7</sup> a 50:50 split between visual and physical roll provided the most realistic perception of roll motion. More recently,<sup>8</sup> the physical roll motion was scaled to 25%, while the visual roll was not scaled (i.e. 100%) with positive results in terms of simulator realism and presence. In Shahar et al.,<sup>9</sup> the participants of a motorcycle simulator experiment were asked to tune the visual and physical roll, resulting in visual roll close to 100% with a physical roll between 40% and 85% of the motorcycle roll, depending on vehicle velocity and turning radius. The present study adopts an approach based on motion perception, where the physical roll motion was used to render specific forces at the rider's head, while visual roll was not modified (i.e. visual gain of 100%). Due to their limited stroke, simulators cannot reproduce sustained accelerations. Here the simulator motion was adapted to produce a realistic direction of the specific force. As the specific force on two-wheeled vehicles is largely aligned with the frame, the adopted physical roll was limited with respect to the roll of an actual vehicle.

Another challenge in the rendering of vehicle motion in a riding simulator is the reproduction of visual cues. In many existing riding simulators a large screen<sup>10–13</sup> or a multiple screen<sup>14</sup> setup was used, while in other cases a Head Mounted Display (HMD) was adopted.<sup>8,15</sup> In this study a HMD with stereo vision and head tracking system was adopted, as it was also used in the study presented in Kováčsová et al.<sup>4</sup> with positive results in braking conditions. In the current test condition, with

the HMD many participants had difficulties controlling the motorcycle and experienced motion sickness. Hence a screen display was extensively evaluated instead.

Regarding the simulator steering feel, different control loading approaches have been used to render the exchange of forces between the vehicle steer and the rider of a motorcycle simulator. In a low-cost motorcycle simulator a torsional spring was used to provide a torque proportional to the steering angle.<sup>14</sup> In Westerhof et al.<sup>8</sup> an admittance control was implemented, where the torque applied by the rider was fed to the model and the resulting steering angle was used to control the position of the steering motor while limiting its torque. In the current study, a speed dependent control was adopted. At very low speed (between 0 and  $0.5 \text{ ms}^{-1}$ ) the torque applied to the steering was proportional to the steering angle, effectively simulating a torsional spring. For higher riding speed (above  $3 \text{ ms}^{-1}$ ) a more advanced torque feedback control was adopted, where the steering angle imposed by the rider and its derivative are used, together with the current vehicle speed and vehicle roll and roll rate, to compute the torque that is applied at the steer. In the speed range in between these situations (between  $0.5$  and  $3 \text{ ms}^{-1}$ ) a speed dependent gain was used to fade out one control strategy and fade in the other in a continuous manner.

Previous studies have considered the development and evaluation of riding simulators, but so far all of them focused on motorcycle maneuvering at high speed (i.e. above  $10 \text{ ms}^{-1}$ ), where the motorcycle vehicle dynamics become intrinsically stable or is easily stabilized by the rider.<sup>16</sup> In contrast, this study focused on the subjective evaluation of a motorcycle riding simulator specifically for low speed maneuvering (i.e. between 0 and  $10 \text{ ms}^{-1}$ ).

The main research question of this study is whether the developed motorcycle simulator provides an adequate reproduction of a real vehicle, both in terms of perceived realism and behavioral fidelity in low speed maneuvers, including cornering. Perceived realism is evaluated both after and during simulator trials, by means of questionnaires and a continuous evaluation of realism.<sup>17</sup> Behavioral fidelity is evaluated by comparing the performance of the subjects of this study, driving a set of maneuvers, with the performance of a test rider on a real instrumented motorcycle conducting the same maneuvers. The performance is evaluated in terms of the resulting vehicle speed profile and vehicle trajectory. Additionally, the effects of simulator platform motion on both perceived realism and behavioral fidelity is evaluated.

## Method

### *Riding scenario*

The riding scenario presented to the experiment subjects is very similar to the scenario used for the experimental validation of the motorcycle model used in

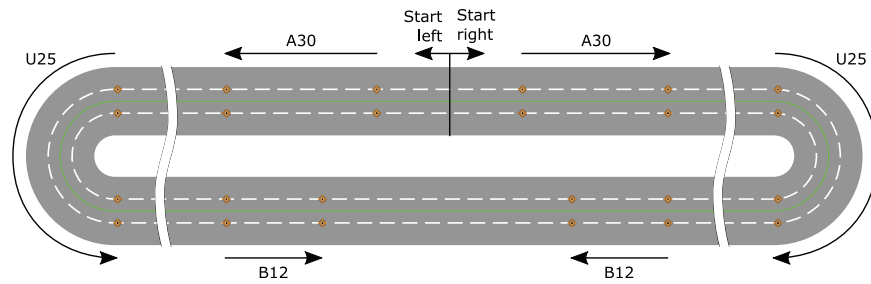


**Figure 1.** Road track used for the experiment. The motorcycle always started in the middle of the top road, heading left or right depending on the initial direction of the turn. The straight parts have been shortened for representation.

Grottoli et al.,<sup>3</sup> where the test data acquired on a real motorcycle were used to validate simulation results. The maneuvers used for model validation were selected to be reproduced here:

- A30: accelerating from standstill to  $30 \text{ km h}^{-1}$  ( $8.3 \text{ ms}^{-1}$ ),
- U25: constant turn with 10.5 m radius performed at  $25 \text{ km h}^{-1}$  ( $6.9 \text{ ms}^{-1}$ ), and
- B12: braking from  $30 \text{ km h}^{-1}$  ( $8.3 \text{ ms}^{-1}$ ) to standstill in 12 m.

In the experiment these maneuvers resulted in accelerations up to  $3 \text{ ms}^{-2}$  (A30),  $4.5 \text{ ms}^{-2}$  (U25), and  $3 \text{ ms}^{-2}$  (B12).

When the experiment started, the participants could see themselves sitting on a standstill motorcycle in a virtual environment. The road on which they were driving was divided in three lanes, 2 m wide each, with the vehicle starting in the middle one. The middle lane also included a green center line which indicated the ideal trajectory that they had to follow. A schematic of the road track created for the experiment is shown in Figure 1.

The first maneuver that they had to reproduce was the acceleration maneuver, which started a few meters ahead of their starting position in the virtual environment. The beginning and the end of the target maneuver was indicated with traffic cones on the virtual road. The second maneuver was the constant turn (left or right, alternatively) indicated also by traffic cones at the beginning and at the end. The third maneuver was the braking to standstill. The target beginning and the stopping locations were indicated using cones.

In-between maneuvers, a 200 long straight road was placed to allow the participants to align on the center of the lane and get to the correct speed. The execution of these three maneuvers in series was defined as a “run.” After the final maneuver (braking) the motorcycle was automatically repositioned to start a new run. The run could start with a right or a left turn, alternating after each run. The execution of three consecutive runs was defined as a “trial.”

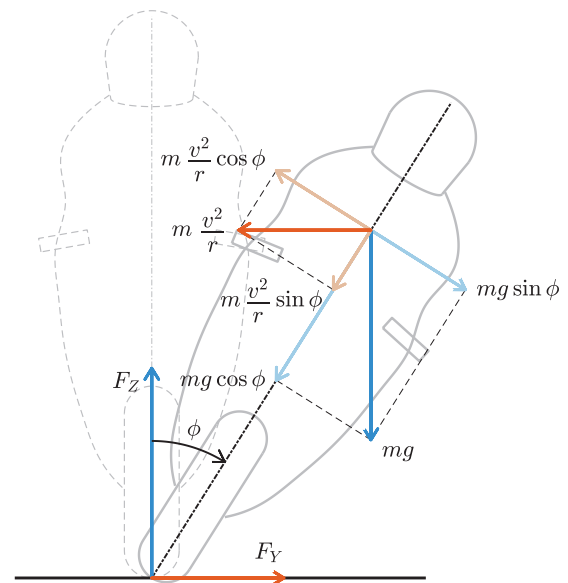


**Figure 2.** Physical and inertial forces acting on the motorcycle and the rider while leaning in a right turn in steady state conditions (rear view).

### Motion cueing

This study adopted an approach based on motion perception to render the roll motion to the riders of the simulator. It is possible to analyze both physical and inertial forces acting on the motorcycle in steady-state cornering, assuming that the rider body does not move with respect to the vehicle and that the rider is in line with the motorcycle.

A scheme of a motorcycle performing a right turn seen from behind is shown in Figure 2, where the masses of the rider and the vehicle are lumped as one. In Figure 2, the subscripts *Y* and *Z* are used to indicate quantities in lateral and vertical direction in the ground reference frame, while the subscripts *y* and *z* indicate quantities in lateral and vertical direction in the motorcycle reference frame. The motorcycle lean angle is noted as  $\phi$ ,  $m$  is the sum of the mass of the motorcycle and the mass of the rider and  $g$  is the gravitational acceleration. The sum of front and rear tires' lateral and vertical forces are noted as  $F_Y$  and  $F_Z$ , respectively.

From the equilibrium of forces, the lateral ( $a_y$ ) and vertical ( $a_z$ ) accelerations acting on the rider can be computed:

$$a_y = g \sin \phi - \frac{v^2}{r} \cos \phi = 0, \quad (1a)$$

$$a_z = g \cos \phi + \frac{v^2}{r} \sin \phi. \quad (1b)$$

The lateral acceleration in a steady state turn depends on the leaning angle, velocity  $v$  and turn radius  $r$ . In the reference frame of the rider and in steady state conditions, if it is assumed that the rider is not moving with respect to the motorcycle, the total lateral acceleration will be zero. In the same reference frame, but in vertical direction, both centrifugal and gravitational accelerations are oriented downwards and their resultant pushes the rider into the motorcycle seat. The accelerations computed using Equations 1a and 1b, together with longitudinal acceleration and angular velocities obtained from the solution of the motorcycle model act as inputs to the Motion Cueing Algorithm (MCA) which commands the platform motion.

The MCA adopted in this study is an algorithm by MOOG, provided together with their motion system. It is based on a classical motion cueing algorithm with adaptive washout.<sup>18</sup> The MCA parameters were tuned to reproduce the accelerations perceived by the rider. The intent was to optimize the motion cueing for the ideal maneuvers. This way, when the participants were improving their performance, they would obtain the most realistic motion experience possible with the adopted motion system and cueing algorithm. Additional details on the adopted algorithm, as well as the motion cueing parameters, can be found in Grotoli.<sup>19</sup>

To evaluate the effects of motion, two different conditions were tested:

- M: motion computed using a filter-based MCA, and
- NM: no motion.

In both conditions, speed-dependent road rumble was added.

### Dependent measures

In order to answer the research question of this study, four classes of metrics were defined. The first class involved metrics of riding performance that can be directly compared with the data acquired on a real vehicle performing the same maneuvers. These objective metrics were complemented with three types of subjective evaluation metrics. The second class is a continuous measure of realism given by the subjects of the experiment. The third class measured simulator

presence based on a questionnaire after the experiment. The fourth class measured simulator sickness.

**Performance metrics.** The rider performance metrics computed for this study are based on lateral position and longitudinal velocity of the vehicle. Lateral deviation of the vehicle with respect to the prescribed path was considered as an error and its sum was computed during the execution of each maneuver. The velocity of the simulated vehicle during acceleration and braking was directly compared with the experimental data acquired on a real instrumented motorcycle, where a test rider performed the same maneuvers.<sup>3</sup> For the turning maneuver the ideal speed was considered to be constant. The deviation from this ideal speed was computed as error and integrated over the execution of the maneuvers.

Position and velocity errors for each maneuver were computed as:

Acceleration performance:

$$\left\{ \begin{array}{l} err_{pos} = \sum_{i=1}^N |(y_i - \hat{y}_{A30})(x_i - x_{i-1})| \\ err_{vel} = \sum_{i=1}^N \frac{|v_i - \hat{v}_{A30,i}|}{|x_i - x_{i-1}|} \end{array} \right. \quad (2a)$$

$$\left\{ \begin{array}{l} err_{pos} = \sum_{i=1}^N |(y_i - \hat{y}_{B12})(x_i - x_{i-1})| \\ err_{vel} = \sum_{i=1}^N \frac{|v_i - \hat{v}_{B12,i}|}{|x_i - x_{i-1}|} \end{array} \right. \quad (2b)$$

Braking performance:

$$\left\{ \begin{array}{l} err_{pos} = \sum_{i=1}^N |(y_i - \hat{y}_{U25})(x_i - x_{i-1})| \\ err_{vel} = \sum_{i=1}^N \frac{|v_i - \hat{v}_{U25,i}|}{|x_i - x_{i-1}|} \end{array} \right. \quad (3a)$$

$$\left\{ \begin{array}{l} err_{pos} = \sum_{i=1}^N |(y_i - \hat{y}_{U25})(x_i - x_{i-1})| \\ err_{vel} = \sum_{i=1}^N \frac{|v_i - \hat{v}_{U25,i}|}{|x_i - x_{i-1}|} \end{array} \right. \quad (3b)$$

Turning performance:

$$\left\{ \begin{array}{l} err_{pos} = \sum_{i=1}^N |r_i - \hat{r}_{U25}| r_i (\psi_i - \psi_{i-1}) \\ err_{vel} = \frac{\sum_{i=1}^N |v_i - \hat{v}_{U25}| r_i (\psi_i - \psi_{i-1})}{\sum_{i=1}^N r_i (\psi_i - \psi_{i-1})} \end{array} \right. \quad (4a)$$

$$\left\{ \begin{array}{l} err_{pos} = \sum_{i=1}^N |r_i - \hat{r}_{U25}| r_i (\psi_i - \psi_{i-1}) \\ err_{vel} = \frac{\sum_{i=1}^N |v_i - \hat{v}_{U25}| r_i (\psi_i - \psi_{i-1})}{\sum_{i=1}^N r_i (\psi_i - \psi_{i-1})} \end{array} \right. \quad (4b)$$

In these equations,  $x$  and  $y$  are the longitudinal and lateral displacement of the motorcycle with respect to  $x_0$  and  $y_0$ , which are the motorcycle planar coordinates at the beginning of each maneuver. The motorcycle velocity during the maneuver is indicated with  $v_i$  while the reference velocity for each maneuver is indicated with  $\hat{v}$ , with the specific maneuver indicated in the subscripts. For the turning maneuver, the instantaneous turning radius  $r_i$  and the angle with respect to the center of the turn  $\psi$  are computed using the motorcycle coordinates. The reference constant lateral displacements for maneuvers A30 and B12 are indicated with  $\hat{y}_{A30}$  and  $\hat{y}_{B12}$ , respectively. The reference turning radius for the maneuver U25 is indicated with  $\hat{r}_{U25}$ . All the sums end at the index  $N$ , which represents the last point

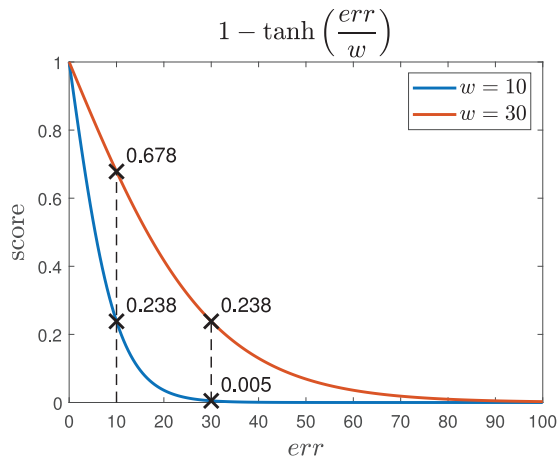


**Figure 3.** Variation of the score when using two different normalization factors. The value of the score remains between 0% and 100%, but as the normalization factor increases, a higher score is associated with the same error value. As an example in the figure, the scores associated with an error of 10 and 30 are shown for the two normalization factors.

in which the motorcycle coordinates are within the pre-defined space of each maneuver.

The computed performances scores for both position and velocity were presented to the subjects of the experiment at the end of each run. Participants were instructed to pursue a high performance score and therefore tended toward the ideal riding scenario, minimizing the dispersion of the data. In order to provide a number that could be quickly interpreted by the participants, the deviation from the ideal trajectory was computed during the simulation and normalized within a range from 0% to 100%, where a score close to 100% is representative of good performance. The normalization was done using a hyperbolic tangent function, including a normalization factor to change the sensitivity of the score to the error variation:

$$\text{score}_{pos} = 1 - \tanh\left(\frac{err_{pos}}{w_{pos}}\right) \quad (5a)$$

$$\text{score}_{vel} = 1 - \tanh\left(\frac{err_{vel}}{w_{vel}}\right) \quad (5b)$$

The normalization factor  $w$  influences the steepness of the score function. Figure 3 shows the trend of the score function for an error value between 0 and 100 with two different normalization factor values.

The normalization factor used was related to physical quantities of the experiment. For the position error for acceleration and braking maneuvers a factor of 10 was used, which is in the order of magnitude of the road width (6 m), while for the position error of the turning maneuver the factor used was 30, which is related to the length of the semi-circular trajectory with

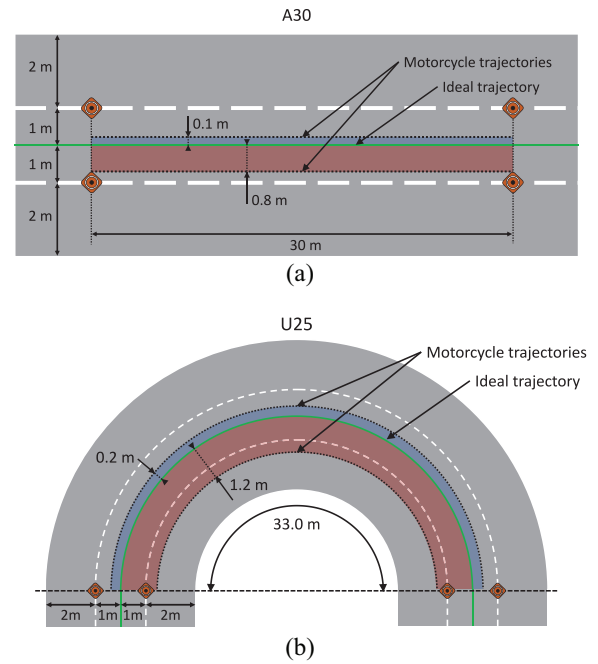


**Figure 4.** Motorcycle trajectories and relative position errors for the calculation of position scores for acceleration and turning maneuver: (a) Position error examples for maneuver A30 and (b) Position error examples for maneuver U25.

a radius 10.5 m (33.0 m). For the velocity scores, the normalization factor used was  $30 \text{ km h}^{-1}$  for all the maneuvers and it was related to the target vehicle velocity of  $30 \text{ km h}^{-1}$  during the experiment. The normalization factor values have been selected with the scope of optimizing the score distribution to use the full range between 0% and 100%.

Examples of position error calculation for the acceleration maneuver A30 are shown in Figure 4(a). Here, two motorcycle trajectories that are parallel to the ideal trajectory but at a certain distance from it are shown. The areas between the trajectories and the ideal trajectory represent the position error. The area colored in blue represents a linear trajectory parallel to the ideal one and at a distance of 0.1 m from it. The position error is computed as the area between the motorcycle trajectory and the ideal trajectory ( $3 \text{ m}^2$ ), which results in a position score of 70.9%. The area colored in red represents the position error relative to a motorcycle trajectory parallel to the ideal trajectory and at a distance of 0.8 m (position error of  $24 \text{ m}^2$ ) with a relative position score of 1.6%. For the braking maneuver B12, the calculations were done in the same way.

Similarly, examples of position error calculations for the turning maneuver U25 are shown in Figure 4(b). Also in this case the position error is computed as the area between the trajectory of the motorcycle and the ideal trajectory. The examples shown in the figure would result in position errors of 6.6 and  $39.6 \text{ m}^2$ , and

position scores of 78.4% and 13.3% for the blue and red area, respectively.

After the execution of the experiment, the performance of the participants was divided in three categories:

- Desired performance: the participant performed the maneuver keeping the motorcycle in the middle lane, maximum lateral deviation from the target path below 1 m on either side,
- Adequate performance: the participant performed the maneuver driving the motorcycle also deviating to the lateral lanes of the road, maximum lateral deviation from the target path below 3 m on either side, and
- Inadequate performance: the participant drove the motorcycle off road while performing the maneuver, lateral deviation from the target path greater than 3 m.

In case of inadequate performance, the position and velocity scores calculated were neglected. The number of times that a participant was not able to obtain desired or adequate performance was analyzed as a measure of difficulty for performing the maneuver. For desired and adequate performances the scores of each participant were averaged per maneuver and per motion condition, where addition of simulator motion is expected to be beneficial to the riding performance.

**Realism.** In order to rate the perceived realism the participants were asked to provide a realism score using a Likert-like scale<sup>20</sup> in the range between 0 and 10, where 0 meant “far from reality” and 10 meant “close to reality.” The participants provided this score by comparing the simulator with their real life experience. They had to provide this score verbally after each maneuver for the entire duration of the experiment. In order to practice with the realism score rating, a training session was performed after the familiarization and before the start of the experiment trials.

The realism scores provided by each participant were averaged per motion condition and per maneuver. The average results over all participants were then computed using the averages of each participant. Although the scale used for the realism score provides ordinal data, in this study it is assumed that the interval between values is the same and therefore the calculation of mean and standard deviation is allowed.<sup>21,22</sup> A higher realism score is expected to be found for the simulator condition with motion, irrespectively of the considered maneuver.

**Simulator presence.** In order to evaluate the simulator presence experienced by the participants during the experiment, a questionnaire was prepared with eight questions selected from a previous study.<sup>23</sup> These questions are meant to measure the major contributing

**Table 1.** Questionnaire evaluating simulator presence for each motion condition.

Nr	Question	Factors
1	To what extent did you feel consciously aware of being in the real world while being on the simulator?	DF
2	To what extent did you feel that you were interacting with the simulation environment?	CF
3	How natural did your interaction with the environment seem?	CF
4	How much did the visual aspects of the environment involve you?	SF
5	How much did the motion aspects of the environment involve you?	SF
6	How well could you concentrate on the assigned tasks or required activities rather than on the mechanisms used to perform those tasks or activities?	DF
7	How much did your experience in the virtual environment seem consistent with your real-world experience?	RF, CF
8	How compelling was your sense of moving around inside the virtual environment?	SF

Factor categories: CF: Control Factors; SF: Sensory Factors; DF: Distraction Factors; RF: Realism Factors.

factors to a sense of presence: Control Factors (CF), Sensory Factors (SF), Distraction Factors (DF) and Realism Factors (RF). Participants were asked to provide an answer between 1 (very low) and 21 (very high/very much) to the questions listed in Table 1. Each participant had to respond to all the questions twice, once for each motion condition. The scale provides ordinal data, but assuming equally-spaced intervals the calculation of mean and standard deviation is allowed.<sup>21,22</sup> The answer of each question per motion condition was averaged for all the participants to analyze the influence of simulator motion on the different factors contributing to simulator presence. A higher mean value is expected when simulator motion is active, while no assumptions are made with respect to dispersion.

**Simulator sickness.** Simulator sickness was measured during the experiment using the Misery Scale (MISC) rating.<sup>24</sup> The rating ranges from no symptoms (0) to vomiting (10) and participants were asked to report their rating in the introduction phase before the beginning of the experiment, after familiarization and training and after each trial. If at any moment during the experiment the MISC rating would reach a value of 6 or higher, the experiment was interrupted and the ongoing scenario was not considered in the analysis.

### Participants

The 12 participants involved in the experiment were recruited from the employees of Siemens Digital Industries Software in Leuven (Belgium), where the motorcycle simulator is located. All participants were



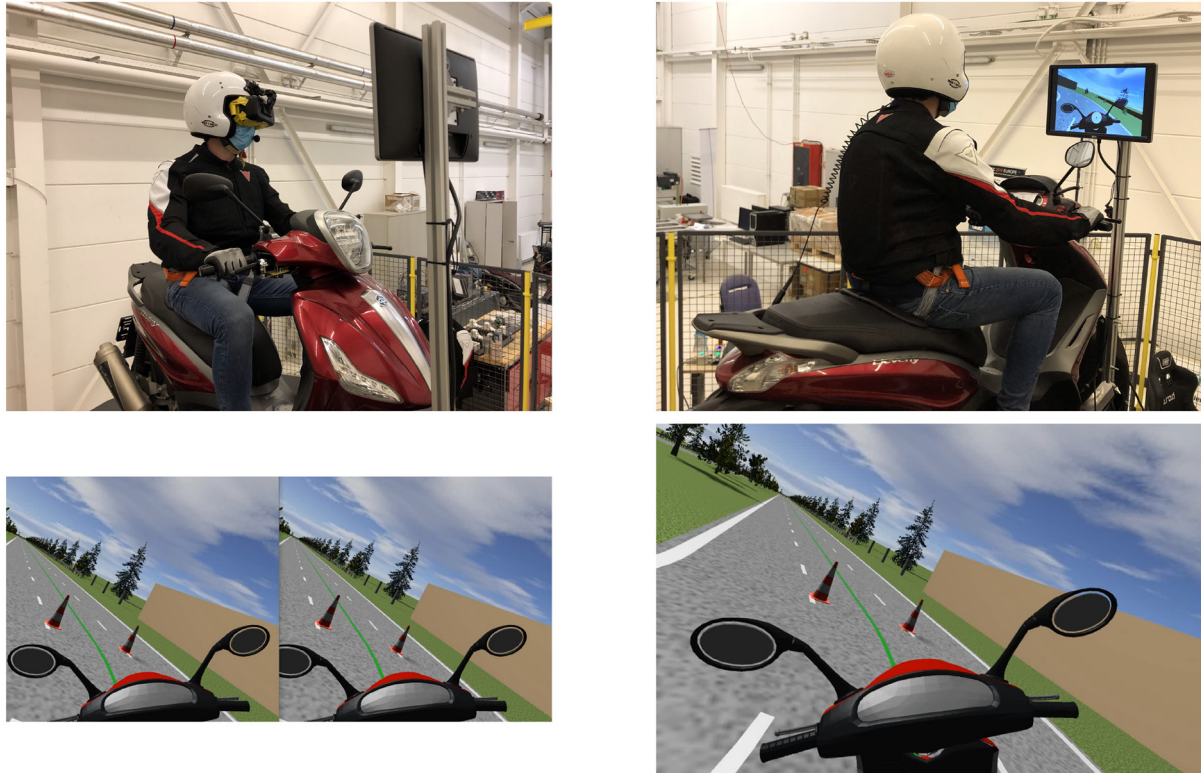


**Figure 5.** The motorcycle simulator using Head Mounted Display (left) and screen (right) to present the driving environment. The lower images represent a screen shot from the turning maneuver.

male with average age of 35.8 years (SD 8.7), and all have a motorcycle driving license (AM, A1, or A). In the 12 months previous to the experiment, half of them reported to have never driven a motorcycle, the other half reported to have driven between once a month and a few times per week.

### *Riding simulator*

The experiment was conducted on the “MOTORIST” motorcycle riding simulator. The simulator consist of a Piaggio Beverly 350 cc motorcycle mock-up mounted on top of a six degrees of freedom MOOG motion system.<sup>4</sup> A HMD integrated in a motorcycle helmet was used to provide stereo vision with visual roll and an infrared camera position in front of the rider was used to track the head motion of the rider. The setup is shown in Figure 5 (left), where the tracking camera was attached to the vertical pole mounted in front of the motorcycle.

The motorcycle was instrumented with sensors to measure the rider inputs of steering, throttle and independent front and rear braking. The steering column was instrumented with an electric motor to provide torque feedback at the handlebar and a rotary encoder to measure the steering angle. The throttle was measured using an encoder mounted on the throttle body of the motorcycle. Braking action was measured independently for front and rear brakes by means of encoders measuring the braking lever’s angle. Throttle

and braking signals were sent to a combined powertrain and braking system model to compute the traction and braking torques to apply to the motorcycle model’s wheels. The steering angle was sent to a lateral controller algorithm responsible for calculating the steering torque that was applied to the motorcycle model. The steering angle imposed by the rider was sent to a lateral controller algorithm responsible for calculating the steering torque that was applied to the motorcycle model. From the motorcycle model, the reaction steering torque was extracted and applied to the simulator handlebar. This torque also included countersteering torque.<sup>3</sup> To stabilize the motorcycle at standstill, the roll dynamics were augmented with dedicated lateral controller. This augmentation was only effective between standstill and  $0.5 \text{ ms}^{-1}$  and phased out at  $3.0 \text{ ms}^{-1}$ . The motorcycle model used was corresponding to the physical motorcycle used for the simulator mock-up and it was validated for the maneuvers executed in this study. A detailed description of the model, subsystems and controls and its validation can be found in.<sup>3</sup>

### *Procedure*

Before the beginning of the experiment, each participant completed an intake questionnaire and was given a document with a description of the experiment, including a set of instructions for the correct execution of the experiment. After reading the experiment description, the



experimenter would answer all questions raised by the participants and then briefly summarize the instructions using the same vocabulary as in the written document and using the same explanation for each subject. Subsequently, the participants had to sign a consent form and provide a preliminary MISC rating.

The participants were then escorted to the riding simulator and helped to wear the protective equipment (safety harness, protective vest, and helmet). Participants started with a familiarization trial to get acquainted with the system. During the familiarization they could drive along the predefined path and attempt to perform the experiment maneuvers, but their performance was not evaluated and they did not have to provide any realism score.

Following the familiarization, they had a training trial. During the training they performed the predefined maneuver and they were also asked to provide a realism score after each maneuver. This score was not considered in the results and was only used to let the participant get used to provide this score at the right time. Both familiarization and training trials were performed with the no motion (NM) condition for all the participants.

After the training, three identical trials with one motion condition were performed. After each trial, participants were asked to provide a rating on the motion sickness, measured using the MISC rating, and at the end of the third trial, the participants were asked to step out of the simulator and fill in a presence questionnaire to evaluate the first motion condition. After a 10 min break, the participants performed the remaining three trials of the experiment with the other motion condition. Also in this case, a MISC rating was requested after each trial, and at the end of the last trial, the participant filled in a final presence questionnaire on the second motion condition. Each participant performed a total of 18 repetitions of each maneuver, nine for each motion condition. The order in which the motion conditions were presented was selected to have half of the participants starting with motion and the other half without. The overall duration of the experiment was approximately 90 min per participant according to the timeline reported in Table 2.

The study was approved by the TU Delft Ethics Committee (Ethics application no. 515, 2018).

## Results

### Replacing the HMD with a screen

The first 10 participants of the experiment used the HMD as visualization device. Only three of them managed to complete the experiment, for the others the experiment had to be interrupted due to inability to drive the motorcycle or motion sickness. These riders were mostly controlling the handlebar too aggressively, resulting in the impossibility to drive in a straight line or control the heading direction. From the feedback

**Table 2.** Experiment timeline.

Introduction	
Intake questionnaire	20 min
Experiment description	
Consent form	
MISC rating	
Familiarization	
NM motion condition	10 min
MISC rating	
Training	
NM motion condition	5 min
Realism score practice	
MISC rating	
3 Trials	
One motion condition	20 min
Realism score measurement	
MISC rating after each trial	
Presence questionnaire	
Break	10 min
3 Trials	
Other motion condition	20 min
Realism score measurement	
MISC rating after each trial	
Presence questionnaire	
Conclusion	5 min
Total	90 min

collected during post-experiment debriefing, they reported issues with the steering control.

The steering angle that was visualized in the HMD was different from the physical steering angle imposed by the driver. At very low speeds (below  $0.5 \text{ ms}^{-1}$ ), the physical steering angle was shown, while at higher speeds (above  $3 \text{ ms}^{-1}$ ) the steering angle of the motorcycle model was visualized. In-between, a speed-dependent gain coefficient was used to smoothly fade between these behaviors, resulting in inaccurate visual reproduction of the handlebar angle. None of the participants mentioned this in their feedback.

To proceed with the experiment, the HMD was replaced by a screen, mounted in front of the motorcycle, which moved together with the motion platform. The adapted setup is shown in Figure 5 (right). With the modified setup, 12 participants were invited to the experiment and all of them were able to complete the study. Three of these participants had started the familiarization with the HMD but interrupted it within few minutes. Therefore, learning from the previous test was considered minimal.

### Time histories compared with real measurements

The average motorcycle velocity profile for all participants and for each motion condition was computed and compared with the reference maneuvers in

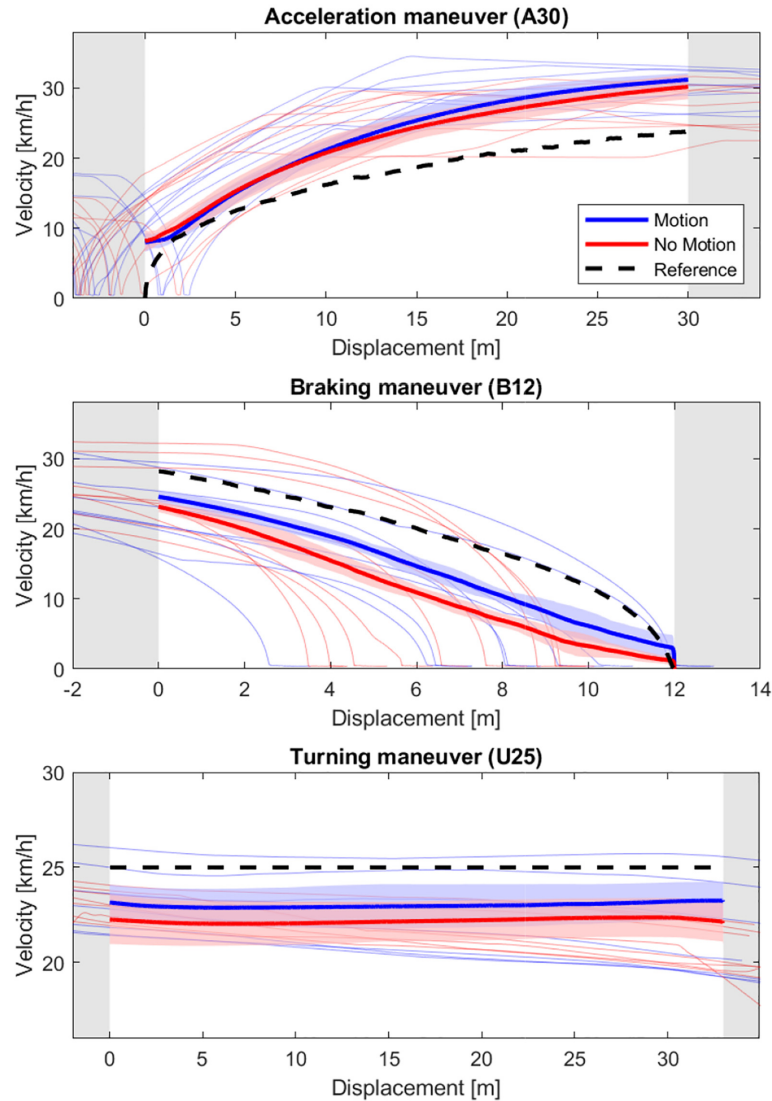


**Figure 6.** Velocity over distance for the experiment maneuvers. The black dashed line indicates the reference profile, blue and red lines the averaged velocity profile for all the participants and shaded areas the interquartile range for motion and no motion condition. Thin lines are velocity profiles of a representative participant for all trials.

Figure 6. The averaged velocity profile for the acceleration maneuver does not start from zero. This is due to the fact that during the trial the motorcycle was repositioned a few meters before the beginning of the maneuver and participants had to drive to the beginning and stop before the start. In some cases, the participants started accelerating before the correct start position and in some other cases, participants started after this position, resulting in an initial averaged velocity higher than zero. This effect can be seen in the velocity profiles of a representative participant for which all the velocity profiles are plotted in Figure 6 (top). The final velocity during the acceleration maneuver is close to  $30 \text{ km h}^{-1}$  for both motion conditions. The reference velocity profile that was measured in experimental conditions does not reach the target speed of  $30 \text{ km h}^{-1}$ , although the instructions provided to both test rider and participants of the simulator

experiment were identical. This indicates that it is easier to reach the ideal final velocity on the simulator rather than on the real vehicle.

For the braking maneuver, the averaged velocity of the motorcycle started to drop before the beginning of the maneuver, resulting in a motorcycle velocity starting below the reference. The shape of the averaged velocity profile is also distorted and differs from the reference. This is due to the averaging in the last part of the maneuver, where for some of the trials the velocity was already at zero (see the velocity profiles for a representative participant in Figure 6 (middle)). For this maneuver it can be seen that with motion, the velocity profile is closer to the reference.

The velocity profile for the turning maneuver was always below the reference value of  $25 \text{ km h}^{-1}$ , with a somewhat higher average value for the condition with simulator motion, as shown in Figure 6 (bottom). This

**Table 3.** Minima, maxima, means, standard deviations for realism and riding performance metrics, and results of paired sample t-tests for the effect of motion.

	M			NM			t (df)	p
	Min	Max	Mean (SD)	Min	Max	Mean (SD)		
<b>Acceleration (A30)</b>								
Realism	4.0	10.0	6.87 (1.61)	0.0	8.0	5.62 (1.96)	1.8 (11)	0.092
Pos. score	0.0	93.0	20.89 (24.19)	0.0	95.7	27.75 (28.21)	-1.3 (11)	0.214
Vel. score	26.7	84.6	51.06 (13.05)	26.9	83.4	54.21 (13.96)	-0.7 (11)	0.491
<b>Braking (B12)</b>								
Realism	2.0	10.0	6.71 (1.88)	1.0	8.0	5.19 (2.17)	1.9 (11)	0.068
Pos. score	7.2	97.2	63.43 (23.24)	6.6	98.7	74.61 (20.78)	-2.5 (11)	<b>0.021</b>
Vel. score	0.0	94.0	37.98 (27.03)	0.0	91.9	28.56 (26.57)	2.5 (11)	<b>0.019</b>
<b>Turning (U25)</b>								
Realism	1.0	10.0	6.74 (1.70)	2.0	9.0	6.13 (1.69)	0.9 (11)	0.365
Pos. score	2.9	83.8	33.46 (22.41)	5.0	92.1	37.84 (21.88)	-0.9 (11)	0.382
Vel. score	93.2	100.0	97.51 (1.68)	92.8	99.9	97.55 (1.65)	-0.3 (11)	0.763

p Values < 0.05 are reported in boldface.

result is in opposition with the results obtained for the acceleration maneuver, where the velocity of the vehicle was always above the reference. This suggests that the ideal reproduction of the turning maneuver was difficult to achieve on the simulator.

### Riding performance metrics and realism

Simulator realism was positively evaluated with an average score of 6.2, and was higher with motion (6.8 with standard deviation of 1.5 for M and 5.6 with standard deviation of 1.7 for NM condition). However this effect was not significant ( $t(11) = 1.61$ ,  $p = 0.123$ , in a paired sample t-test). The results of realism and performance evaluation were first averaged per participant and per motion condition and then represented graphically in box plots in Figure 7. In order to evaluate significance of the effect of motion, a paired t-test was performed, see Table 3.

For the acceleration maneuver A30, results shown in Figure 7 (top). The effects of motion were not significant for this maneuver, with a minor influence on realism, for which the mean value is slightly higher with motion. The position scores obtained are quite low, with an average value around 20%, which represents an error value of  $11.0 \text{ m}^2$ , resulting in an average deviation from the ideal trajectory of 0.37 m for 30 m of acceleration. Results for the braking maneuver B12 are shown in Figure 7 (middle). Here, the effect of motion is significant for both position and velocity scores. In particular, the position score is significantly higher for the NM condition (10.5%), while the velocity score is significantly higher for the M condition (8.8%).

For the turning maneuver U25, results are shown in Figure 7 (bottom). The average velocity score for all the participants was always between 95.0% and 99.5%, with a corresponding error between  $1.5$  and  $0.15 \text{ km h}^{-1}$

The small range of these results is explained by the small amplitude of the error value and the normalization factor used for the calculation of this score. In this case, as for the other velocity scores, a normalization factor of 30 was used. As shown in Figure 3, a smaller factor would result in an increased score range for a small error in magnitude. These results were re-scaled using a normalization factor of 1 (instead of 30), resulting in a score range between 9.5% and 85.1% and a similar statistical result ( $t(11) = -0.25$ ,  $p = 0.802$ ) for the difference between motion and no motion condition. Although the updated normalization factor provides a better use of the score range, the numbers shown in Figure 7 were presented to participants during the experiment and were used to adjust performance. Since the normalization factor does not influence the outcome of the analysis, the results with the pre-selected factor are shown.

For the calculation of the performance scores only the maneuvers where participants achieved desired or adequate performance were considered. For inadequate performances, the scores were excluded. The total numbers of inadequate performances for each maneuver, and the percentage of the total number of repetitions, are listed in Table 4, for both screen and HMD visuals.

Overall, no falls or loss of balance were reported during the experiment, and participants were able to successfully reproduce acceleration from standstill and braking to standstill with the help of the balancing control. In terms of deviation from the desired path, participants failed to achieve adequate performances for the acceleration maneuver seven times for each motion condition. For the braking maneuver, one inadequate performance instance with platform motion and three without motion were found. For the turning maneuver, the inadequate performances were 33 for each motion condition.

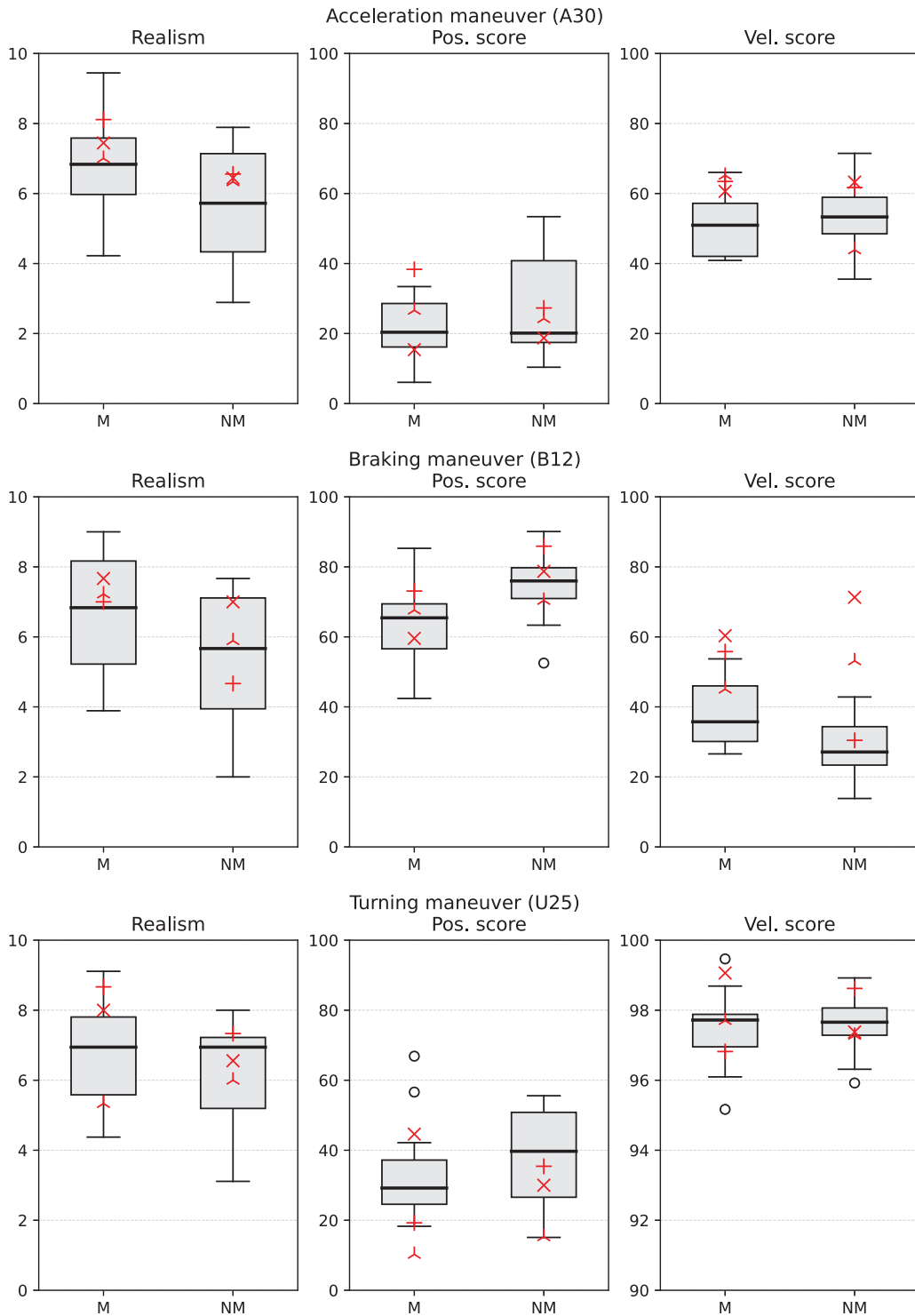


**Figure 7.** Box plot of realism scores, position scores and velocity scores for the acceleration maneuver (top), braking maneuver (middle) and turning maneuver (bottom) grouped by motion condition (M: motion, NM: no motion). *p* values for effects of motion result from a paired sample t-test. Boxes show results with screen. The red markers represent the three participants that completed the experiment using the Head Mounted Display.

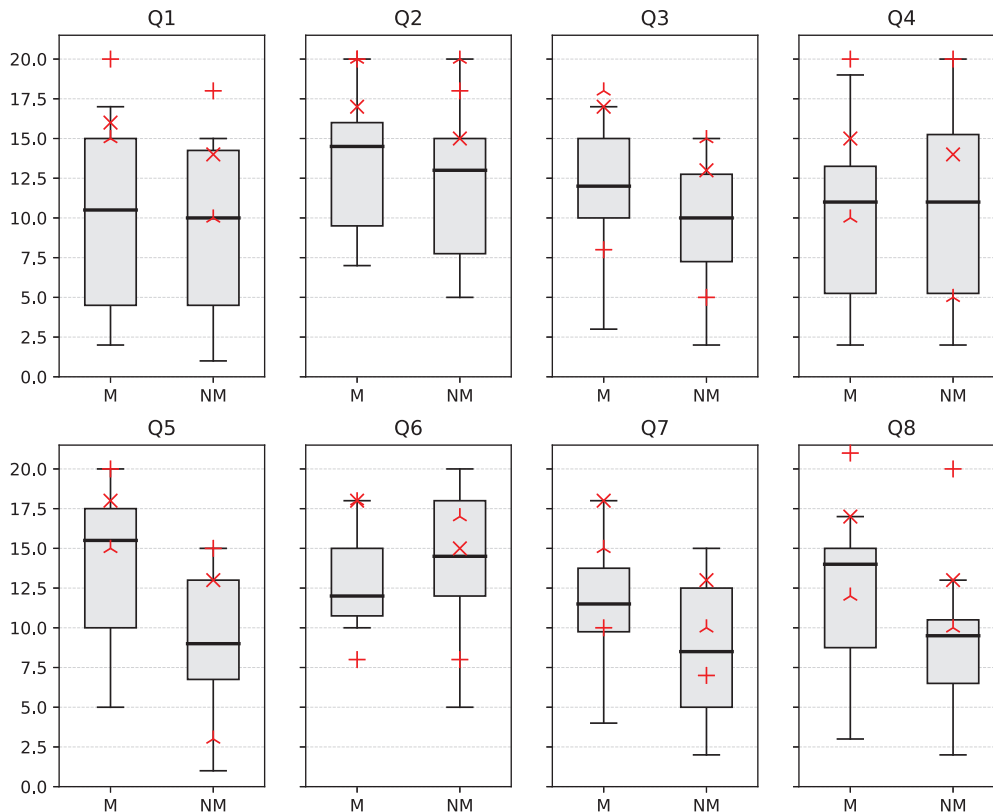
**Simulator presence**

Results from the simulator presence questionnaire are illustrated in Figure 8. Results of a paired t-test are listed in Table 5. Only for Question 5 (“How much did

the motion aspects of the environment involve you?”) a significant effect was found, with participants feeling more present in the virtual environment with simulator motion. The results show that the value is generally

**Table 4.** Number of inadequate performances (failures) for each maneuver per motion condition and percentage of the total number of repetition.

	Screen (12 participants)				HMD (3 participants)			
	M		NM		M		NM	
	Failed	%	Failed	%	Failed	%	Failed	%
Acceleration (A30)	7	6.5	7	6.5	I	3.7	2	7.4
Turning (U25)	33	30.6	33	30.6	II	40.7	8	29.6
Braking (B12)	I	0.9	3	2.8	I	3.7	I	3.7

**Figure 8.** Presence questionnaire results grouped by motion condition (M: motion, NM: no motion).  $p$  values from effects of motion result from a paired sample  $t$ -test. The markers represent the three participants that completed the experiment using the Head Mounted Display.

higher with motion, except for Question 6 (“How well could you concentrate on the assigned tasks or required activities rather than on the mechanism used to perform those tasks or activities?”), where simulator motion results in lower presence.

### Simulator sickness

Results of the self-reported simulator sickness for the experiment using the screen are listed in Table 6, with a comparison between the motion and no motion conditions. The maximum MISC rating value during trials was 2 and it was reported during a trial without motion. The average MISC rating during trials was 0.25 and 0.22 with motion and without motion, respectively. The highest average MISC rating was reported in the introduction phase of the experiment with a value of 0.33.

### Usage of motion envelope

The available motion envelope for the adopted motion platform is 1.00 m in longitudinal translation with  $\pm 22^\circ$  of pitch motion for the reproduction of longitudinal motion. For lateral motion, the motion envelope is 0.92 m in lateral translation with  $\pm 22^\circ$  of roll. In vertical direction, the available motion envelope is 0.76 m.

During the trials where the motion was present, for the reproduction of acceleration and braking maneuvers, the average motion envelope (and standard deviation SD) used was 45.3% (SD 14.0%) in longitudinal translation and 35.1% (SD 3.8%) in pitch rotation. For the turning maneuver, the average used motion envelope was 21.9% (SD 8.0%) in lateral translation and 20.4% (SD 7.0%) in roll rotation. In vertical translation, 79.1% (SD 2.5%) of the available motion envelope was used.

**Table 5.** Minima, maxima, means, standard deviations and results of paired sample t-tests for presence questionnaire.

	M			NM			t (df)	p
	Min	Max	Mean (SD)	Min	Max	Mean (SD)		
Q1	2	17	9.92 (5.62)	0	15	8.92 (5.38)	0.41 (11)	0.683
Q2	7	20	13.08 (4.25)	5	20	11.83 (4.63)	0.69 (11)	0.498
Q3	3	17	11.42 (4.60)	2	15	9.50 (4.50)	1.03 (11)	0.314
Q4	2	19	9.83 (5.87)	2	20	10.33 (6.31)	-0.20 (11)	0.844
Q5	5	20	14.25 (4.94)	1	15	9.08 (4.48)	2.68 (11)	<b>0.014</b>
Q6	10	18	13.00 (2.76)	5	20	14.17 (4.17)	-0.81 (11)	0.428
Q7	4	18	11.75 (4.11)	2	15	8.67 (4.54)	1.74 (11)	0.095
Q8	3	17	11.67 (4.56)	2	13	8.50 (3.42)	1.92 (11)	0.067

p Values < 0.05 are reported in boldface.

**Table 6.** Self-reported simulator sickness for the 12 participants with screen and the three participants with HMD.

	Screen (12 participants)			HMD (3 participants)		
	Min	Max	Mean (SD)	Min	Max	Mean (SD)
Introduction	0	1	0.33 (0.49)	0	1	0.33 (0.58)
Familiarization	0	1	0.17 (0.39)	0	2	1.00 (1.00)
Training	0	1	0.08 (0.29)	0	2	1.00 (1.00)
Trials M	0	1	0.25 (0.44)	0	2	0.33 (0.71)
Trials NM	0	2	0.22 (0.48)	0	3	1.00 (1.00)

## Discussion

To use a motorcycle riding simulator for training purposes at low speeds, validation is needed in representative driving conditions. In this study, simulator realism and behavioral fidelity of a motorcycle simulator are evaluated for acceleration, cornering and braking maneuvers at low speed. The participants of the experiment performed these maneuvers while controlling the vehicle using throttle, brake and steering. At the end of each maneuver, they provided measures of realism while their performances were used to evaluate behavioral fidelity.

### Simulator evaluation

Overall, the simulator can be used to reproduce the targeted maneuvers at low speed. This is based on the analysis of the results obtained in the conducted experiment with screen visualization. Results obtained with HMD are not satisfactory as discussed in a following subsection.

From the performance analysis it can be seen that all the participants were able to perform the maneuvers, with the turning maneuver resulting to be slightly more difficult, with 30.6% inadequate performances exceeding the intended path with more than 3.

As shown in Figure 6 (top and bottom), the targeted beginning of the acceleration and braking maneuvers was not easily identified by the participants, as the reference point was placed in the center of gravity of the motorcycle and the only visual reference available to them were the cones placed on the road, which were not clearly visible once passed with the front wheel. This

resulted in a somewhat scattered distribution of the initial point of the acceleration and braking maneuvers.

From the analysis of the velocity profiles for the acceleration maneuver, it can be seen that the participants were able to accelerate to exactly  $30 \text{ km h}^{-1}$ , while in the real vehicle experiments, giving the same instructions to the rider, the velocity reached at the end of the maneuver was lower (see Figure 6). One of the possible explanations for this could be the fact that the speedometer in the riding simulator was placed close to the center of the field of view, allowing for a better speed control than on a real motorcycle, where the speedometer is placed in a lower position, making it harder for the rider to check if the exact speed was reached. Another possible explanation is related to the limited field of view of the visualization screen used during the experiment. A previous study<sup>25</sup> has found a correlation between the field of view and the perception of speed. In this study, the limited field of view could have influenced the participants to drive faster during the acceleration maneuver, although this did not occur in the other two maneuvers performed during the experiment.

### Effects of simulator motion

Riding performance analyses show small effects of motion only for the braking maneuver, with a positive influence on velocity score and a negative effect on position score. A minor effect was found in the presence questionnaire, where the results for the question related to the motion aspects of the simulation were found to be significantly higher when physical motion



was present. Similar results were found in a previous experiment on the same simulator<sup>4</sup> in longitudinal-only scenarios and on another simulator<sup>8</sup> in high speed longitudinal and lateral scenarios.

Given the multiple number of *t*-tests performed in the analysis of the results shown in Figures 7 and 8, the chance of type I errors is increased. This would mean that the tests that resulted in a significant difference might be false positives, where the null hypothesis was wrongly rejected. A Bonferroni correction<sup>26</sup> could be applied to take this effect into account. These correction adjusts the critical *p*-value to take into account the number of repeated *t*-tests, lowering the threshold from 5% to 0.3% (5%/17 *t*-tests). This correction would make the rejection of the null hypothesis invalid for all the tests performed, and consequently indicate no significant differences between the motion and no motion conditions.

Another study analyzed the effect of motion on a riding simulator at higher speed.<sup>27</sup> They found that the addition of motion was beneficial to achieve higher simulator behavioral fidelity and presence. But when participants were asked to rank which sensory cue was mostly influencing their performance, the majority indicated that motion was the least contributing cue of all presented. Investigations on the effects of motion can be found in literature studies on car driving simulators. In the reproduction of highly dynamic lateral maneuvers, the effect of motion was found to be significant in terms of both behavioral fidelity and presence in different studies.<sup>28,29</sup> Another study investigated effects of motion while turning on a car driving simulator,<sup>30</sup> and showed that differences in driving performance are not significant with respect to the adopted motion cueing strategy, although motion cueing had an impact on perceived realism. Similarly, in this study it was found that the motion has a small impact on performance (with the exception of the braking maneuver) but a significant impact on the motion element of perceived simulator realism. We conclude that, depending on the task assigned to the participant of the simulator study, the influence of motion cueing is not a key factor to achieve a sufficient level of behavioral fidelity, while it has an impact on the realism perceived on the simulator.

The limited motion range of 1.00 m in longitudinal and 0.92 m in lateral direction obviously limited the reproduction of sustained accelerations, and benefits of platform motion may become more significant with larger motion ranges.

### Considerations on visualization technologies

Regarding the adopted simulator visuals, the original simulator configuration adopted a HMD as used in Kováčová et al.<sup>4</sup> with positive results for the reproduction of longitudinal maneuvers. In this experiment, also lateral maneuvering was added, and the HMD was found to be quickly unusable for 7 out of 10 participants due to induced motion sickness or simply due to inability to drive. The results obtained by the three

participants who completed the study using the HMD were reported for the sake of completeness with the other results as red markers in Figures 7 and 8 and in Table 4. However, given the limited sample, no further conclusions can be drawn from these results.

The modification of the simulator to adopt a screen with static background resulted in the elimination of motion sickness occurrence. This can be explained with the rest frame theory found in literature,<sup>31,32</sup> which states that creating a static visual background consistent with the absence of inertial motion information reduces motion sickness induced by visual stimulation. This result is in contrast with a previous study,<sup>8</sup> however, where a HMD was used in a motorcycle simulator to reproduce high speed maneuvers without inducing motion sickness. The occurrence of motion sickness when using the HMD can be therefore explained by the rest frame theory. However, it cannot be excluded that an HMD can be successfully adopted in a motorcycle simulator at low speeds. Improvements may be found using more advanced HMDs in combination with improved control techniques for both visual and visual/motion combinations.

### Conclusions

An experiment was performed to validate a motorcycle riding simulator in the speed range between 0 and 10 ms<sup>-1</sup>. Participants were asked to reproduce a set of maneuvers which were previously performed on a real motorcycle. Results show that the selected maneuvers can indeed be reproduced on the motorcycle riding simulator, and the overall level of realism measured during the experiment is sufficient (6.2 overall on a scale from 1 to 10, 6.8 with motion, and 5.6 without motion).

In terms of behavioral fidelity, the comparison between the simulator and experimental results shows good agreement, with a limited, positive, influence of the simulator motion. Only for the braking maneuver this effect was significant, which indicates that for this maneuver the use of motion is beneficial to reproduce the real-life experience and performance. Motion also had a positive effect on simulator presence, significantly increasing the feeling of being involved in the virtual environment.

### Declaration of conflicting interests


The author(s) declared no potential conflicts of interest with respect to the research, authorship, and/or publication of this article.

### Funding

The author(s) disclosed receipt of the following financial support for the research, authorship, and/or publication of this article: This work has been funded by the European Union's Seventh Framework Programme through the international consortium MOTORIST

(Motorcycle Rider Integrated Safety) agreement No. 608092.

## ORCID iD

Marco Grottoli  <https://orcid.org/0000-0002-7542-9763>

## References

- Allen RW, Park GD and Cook ML. Simulator fidelity and validity in a transfer-of-training context. *Transp Res Rec J Transp Res Board* 2010; 2185(1): 40–47.
- Pinto M, Cavallo V and Ohlmann T. The development of driving simulators: toward a multisensory solution. *Trav Hum* 2008; 71(1): 62–95.
- Grottoli M, Celiberti F, van der Heide A, et al. Motorcycle multibody model validation for human-in-the-loop simulation. In: *Driving simulation & virtual reality conference & exhibition*, 2019.
- Kováčová N, Grottoli M, Celiberti F, et al. Emergency braking at intersections: a motion-base motorcycle simulator study. *Appl Ergon* 2020; 82: 102970.
- Kageyama I. Development of a riding simulator for two-wheeled vehicles. *JSAE Rev* 2002; 23(3): 347–352.
- Cossalter V, Lot R and Rota S. Objective and subjective evaluation of an advanced motorcycle riding simulator. *Eur Transp Res Rev* 2010; 2(4): 223–233.
- Guth S, Geiger M, Will S, et al. Motion cueing algorithm to reproduce motorcycle specific lateral dynamics on riding simulators. In: *Driving simulation conference & exhibition*, 2015.
- Westerhof BE, de Vries EJH, Happee R, et al. Evaluation of a motorcycle simulator. In: *Proceedings, bicycle and motorcycle dynamics*, 2019.
- Shahar A, Dagonneau V, Caro S, et al. Towards identifying the roll motion parameters of a motorcycle simulator. *Appl Ergon* 2014; 45(3): 734–740.
- Cossalter V, Lot R, Massaro M, et al. Development and validation of an advanced motorcycle riding simulator. *Proc IMechE, Part D: J Automobile Engineering* 2011; 225(6): 705–720.
- Stedmon AW, Hasseldine B, Rice D, et al. ‘Motorcycle-Sim’: an evaluation of rider interaction with an innovative motorcycle simulator. *Comput J* 2011; 54(7): 1010–1025.
- Miyamaru Y, Yamasaki G and Aoki K. Development of a motorcycle riding simulator. *JSAE Rev* 2002; 23(1): 121–126.
- Guth S. Motorcycle riding simulation to assess instrument and operation concepts and informing riding assistance systems. In: *10th international motorcycle conference*, 2014.
- Savino G, Pierini M and Lenné MG. Development of a low-cost motorcycle riding simulator for emergency scenarios involving swerving. *Proc IMechE, Part D: J Automobile Engineering* 2016; 230(14): 1891–1903.
- Chiyoda S, Yoshimoto K, Kawasaki D, et al. Development of a motorcycle simulator using parallel manipulator and head mounted display. *Proc Int Conf Motion Vibr Control* 2002; 6.1: 599–602.
- Sharp RS. Optimal stabilization and path-following controls for a bicycle. *Proc IMechE, Part C: J Mechanical Engineering Science* 2007; 221(4): 415–427.
- Cleij D, Venrooij J, Pretto P, et al. Continuous subjective rating of perceived motion incongruence during driving simulation. *IEEE Trans Hum Mach Syst* 2018; 48(1): 17–29.
- Chen SH and Fu LC. Predictive washout filter design using the forward kinematics and a kalman filter. In: *2007 IEEE international conference on control applications*, 2007. New York, NY: IEEE. DOI:10.1109/cca.2007.4389267.
- Grottoli M. *Development and evaluation of a motorcycle riding simulator for low speed maneuvering*. Delft: Delft University of Technology, 2021.
- Likert R. A technique for the measurement of attitudes. *Arch Psychol* 1932; 22(140): 55.
- Jamieson S. Likert scales: how to (ab)use them. *Med Educ* 2004; 38(12): 1217–1218.
- Norman G. Likert scales, levels of measurement and the “laws” of statistics. *Adv Health Sci Educ* 2010; 15(5): 625–632.
- Witmer BG and Singer MJ. Measuring presence in virtual environments: a presence questionnaire. *Presence: Teleoperators and Virtual Environments* 1998; 7(3): 225–240.
- Bos JE, MacKinnon SN and Patterson A. Motion sickness symptoms in a ship motion simulator: effects of inside, outside, and no view. *Aviat Space Environ Med* 2005; 76: 1111–1118.
- Pretto P, Ogier M, Bülthoff HH, et al. Influence of the size of the field of view on motion perception. *Comput Graph* 2009; 33(2): 139–146.
- Cleophas TJ and Zwinderman AH. *Statistical analysis of clinical data on a pocket calculator*. Dordrecht: Springer Netherlands, 2011.
- Will S. *Development of a presence model for driving simulators based on speed perception in a motorcycle riding simulator*. PhD Thesis, Julius-Maximilians-Universität Würzburg, 2017.
- Grácio BJC, Wentink M and Valente Pais AR. Driver behavior comparison between static and dynamic simulation for advanced driving maneuvers. *Presence* 2011; 20(2): 143–161.
- Reymond G, Kemeny A, Droulez J, et al. Role of lateral acceleration in curve driving: driver model and experiments on a real vehicle and a driving simulator. *Hum Factors* 2001; 43(3): 483–495.
- Damveld HJ, Wentink M, van Leeuwen PM, et al. Effects of motion cueing on curve driving. In: *Driving Simulation Conference*, 2012.
- Prothero JD, Draper MH, Furness TA, et al. Do visual background manipulations reduce simulator sickness? In: *Proceedings of the international workshop on motion sickness: medical and human factors*, 1997, pp. 18–21.
- Prothero JD. *The role of rest frames invection, presence and motion sickness*. PhD Thesis, University of Washington, USA, 1998.